Characteristics of Backscattering Coefficients over Different Vegetation Land Covers Derived from TRMM/PR

Junichi NAGAOKA[1], Munehisa K. YAMAMOTO[2], and Atsushi HIGUCHI[3]

[1]*Graduate School of Science, Chiba University*
(1-33, Yayoi-cho, Inage-ku, Chiba, 263-8522, Japan), nagaoka@graduate.chiba-u.jp
[2]*Center for Environmental Remote Sensing (CEReS), Chiba University*
(1-33, Yayoi-cho, Inage-ku, Chiba, 263-8522, Japan), mkyamamoto@faculty.chiba-u.jp
[3]*CEReS, Chiba University (1-33, Yayoi-cho, Inage-ku, Chiba, 263-8522, Japan), higu@faculty.chiba-u.jp*

Abstract

The characteristics of backscattering coefficients (σ^0) observed by the Tropical Rainfall Measuring Mission (TRMM) / Precipitation Radar (PR) were investigated for different vegetation covers; evergreen broadleaf forests (ebf), woody savannas, savannas, open shrublands, and grasslands in Africa. For ebf, σ^0 decreases rapidly from nadir to 3°, then the rest of the angles are constant. On the other hand, σ^0 gradually decreases from nadir to 17° for savannas, open shrublands, and grasslands. For woody savannas, σ^0 value for each angle bin in the dry season is similar to that for savannas, but the characteristics of σ^0 in the rainy season is similar to that for ebf. The maximum monthly mean precipitation corresponds to that of σ^0 at nadir and 17° for grasslands and savannas. For grasslands, σ^0 at 3° does not increase that is likely to be saturated from the dry season to the rainy season when Leaf Are Index (LAI) is more than 0.5. Seasonal variations of σ^0 do not clearly correspond to that of precipitation for ebf where LAI is more than 3. It implies that σ^0 at 3° is susceptible to vegetation canopy. It suggests that the combination of 3° and 17° of σ^0 enable to classify vegetation land covers.

Keywords **:** TRMM/PR, backscattering coefficients, vegetation land covers, incident angle dependency, seasonal variation

1. Introduction

Satellite microwave remote sensing has attracted a lot of attention as one of methods for collecting global information on land surface. The Tropical Rainfall Measuring Mission (TRMM) has on board Precipitation Radar (PR) that is the first spaceborne rain radar. The TRMM PR observes backscattering not only from rain particles but also from surface to estimate path integrated attenuation (PIA) by a surface reference technique (SRT) [1]. Thus, it is possible to monitor land surface from surface backscattering coefficient (σ^0) by PR. Some previous studies applied TRMM PR signals for monitoring land surfaces. Seto et al. [2] investigated characteristics of σ^0 by TRMM PR as a basic of soil moisture estimation. Hirabayashi et al. [3] produced a land cover map from σ^0 observed by TRMM PR. Satake and Hanado[4] showed a diurnal variation in σ^0 over the Amazon rain forest, and they concluded that the increase of σ^0 in the early morning is probably caused by dewdrops on leaves. The characteristics of σ^0 over vegetation land covers are however still far from fully understood. The objective of this study is to reveal the characteristics of σ^0 over different vegetation land covers.

2. Data

2.1 TRMM/PR

The TRMM PR employs 13.8 GHz (Ku band) microwave with Horizontal transmit-Horizontal receive polarization[5]. The PR antenna beam scans in the cross-track direction over ±17° that has 220 km swath width. The antenna width of the PR is 0.71° and there are 49 observation angle bins within the scanning angle of ±17° (e.g., the angle bins 1, 25, and 49 correspond to -17°, 0°, and +17°, respectively). The horizontal resolution (footprint size) is 4.3 km at nadir and about 5 km at the scan edge in initial orbit altitude (350 km).

In this study, σ^0 from 2A25 standard product (Ver. 6) were used. In addition, σ^0 under no rain were used if rain flag from 2A23 standard product (Ver. 6) shows "no rain" or "rain possible". The analyzed periods were from 1998 to 2007.

2.2 Precipitation and Leaf Area Index (LAI)

Precipitation data from 3B43 product[6] (monthly 0.25° merged TRMM and other satellites estimation) were used. The Moderate Resolution Imaging Spectroradiometer (MODIS) LAI product (MOD15A2; Version 5) [7] were used. The LAI in MOD15A2 is defined as one sided green leaf

area per area (unit: m^2/m^2). The product is 8-days composite with 1 km resolution. The data were converted from 1 km to 0.25° grid to set the same resolution of the precipitation data.

2.3 Land Cover (IGBP.EcoMap)

The One-Minute Land Ecosystem Classification Product is a global (static map) data set provided by the International Geosphere-Biosphere Programme (IGBP) with an equal-angle rectangular grid at 1-minute resolution. IGBP.EcoMap classifies land covers into 17 categories. The targets in this study are evergreen broadleaf forest (ebf), woody savannas, savannas, open shrublands, and grasslands in Africa. The 5-biomes Africa map is shown in Fig. 1.

2.4 Uniform σ^0

Previous study[4] pointed out that σ^0 mixed both forest and river in the Instantaneous Field Of View (IFOV) of PR is higher than σ^0 that in just forest area. In order to obtain pure σ^0 of land covers such as ebf and grasslands, mixed areas in land covers using IGBP.EcoMap in 5 × 5 pixels (about 5 km × 5 km) was excluded

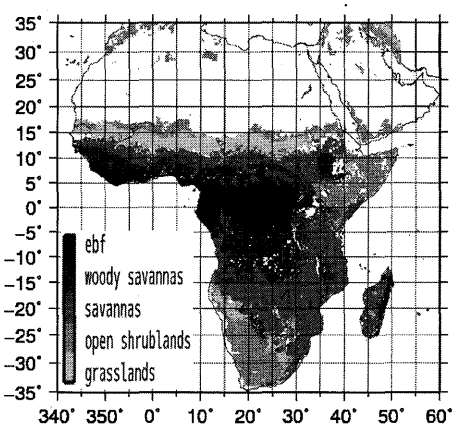

Fig. 1. 0.25° grid 5-biomes map used by IGBP.EcoMap. White pixels display other land covers such as barren and water.

3. Results and Discussion

3.1 Incident Angle Dependency of σ^0 and Seasonal Variations

In order to compare the differences in surface conditions between in the wet and dry seasons, σ^0 every incident angles are investigated. Seasonal variations of σ^0 for different incident angles are also compared to those in precipitation and LAI for 3 vegetation land covers.

3.1.1 ebf (0-5°S, 20-25°E)

σ^0 rapidly decreases from nadir to 3°, then is almost constant (about -2 dB) regardless of the seasons (Fig. 2. (a)). The seasonal variation of σ^0 for all angles is very small (Fig. 2. (b)). σ^0 does not have clear relation both precipitation and LAI.

3.1.2 grasslands (10-15°N, 5-15°E)

σ^0 in dry month decreases from nadir to 5°, and is almost constant from 7° to 10°, then decreases to 17° (Fig. 3. (a)). In contrast, σ^0 in rainy month gradually decreases from nadir to 17°. σ^0 at nadir in grasslands is higher than that in ebf, but σ^0 at more than 10° in grasslands is lower than that in ebf.

The phase at seasonal variation of σ^0 at nadir and 17° is similar to that of precipitation (Fig. 3. (b)). The higher precipitation, the higher soil moisture. This implies that σ^0 is affected by soil moisture depends on precipitation. On the other hand, the month of maximum σ^0 at 3° does not correspond to that of precipitation, when LAI is more than 0.5. It implies that σ^0 at 3° is susceptible to vegetation canopy. In addition, the seasonal variation of σ^0 at 12° is very small.

3.1.3 woody savannas (5-10°S, 20-25°E)

There is the largest difference between σ^0 at more than 10° in the rainy month and those in the dry month in the other vegetation covers (Fig. 4. (a)). The incident angle dependency of σ^0 in the dry month is similar to that for savannas (not shown), but that in the rainy month is similar to that for ebf. Comparing to savannas, land surface in woody savannas in the rainy season are covered by leaves of forests and grass. It shows land surface in the rainy month became rough. There is not clear relation between σ^0 at nadir and both precipitation and LAI (Fig. 4. (b)). However, the seasonal variation of σ^0 at 17° corresponds to precipitation. It implies that σ^0 is affected by soil moisture.

3.2 Cluster Analysis

Figure 5 shows a scatter diagram (feature space) between annual mean σ^0 at 3° and annual mean σ^0 at 17° and the distribution in Africa after the k-means cluster analysis. The dynamic range of σ^0 at 3° is larger than that of σ^0 at 17°, but the most of data of σ^0 at 3° distributes from -2 to 2 dB. As a result, ebfs such as Congo, the West Africa coast, and Madagascar are classified in class 4 (σ^0 at 3° is low and σ^0 at 17° is high). The west sides in Sahel (11-13°N, 5-10°E) are classified in class 3. In contrast, the east sides in Sahel (12-14°N, 15-20°E) are classified in class 2. σ^0 at 17° in the west sides is higher than that in the east sides (not shown). In addition, precipitation in the west sides is higher than that in the east sides (not shown). It implies that soil moisture in the west sides is higher than that in the east sides.

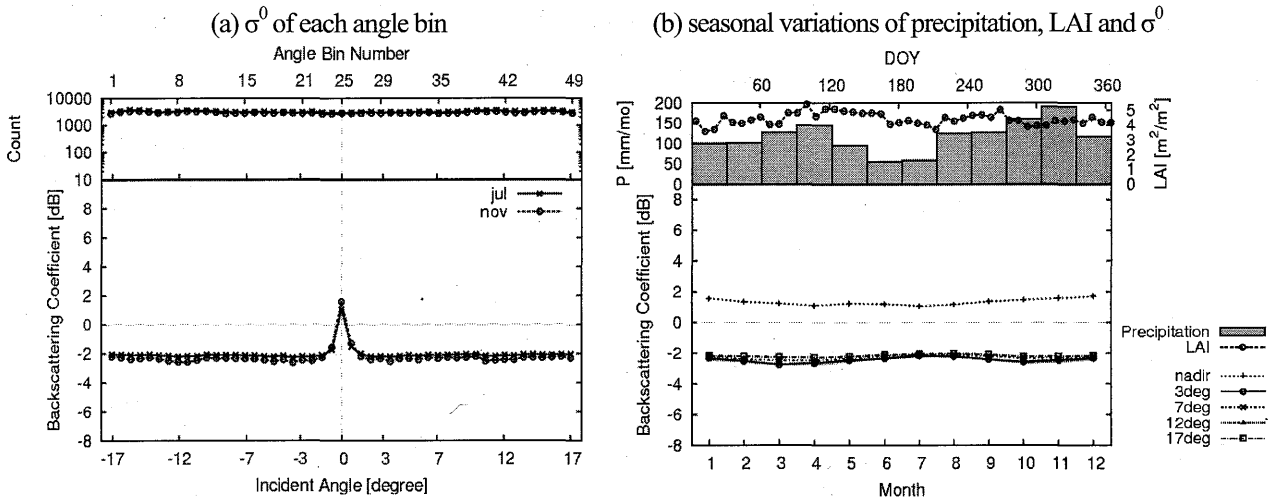

Fig. 2. σ^0 of each angle bin and seasonal variations of precipitation, LAI, and σ^0 for 5 angles for ebf.

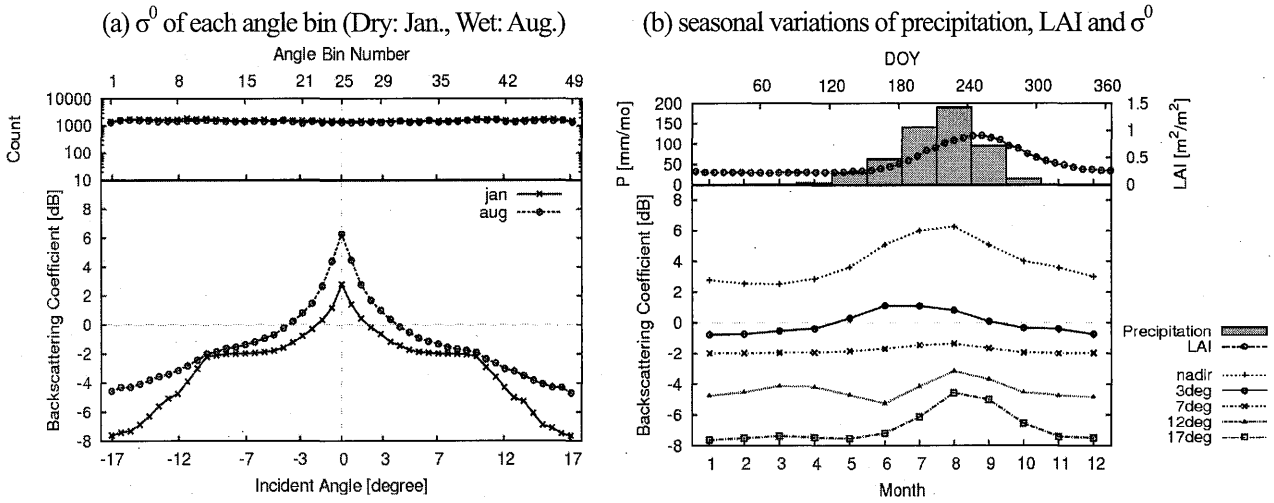

Fig. 3. The same as Fig. 2 but for grassland.

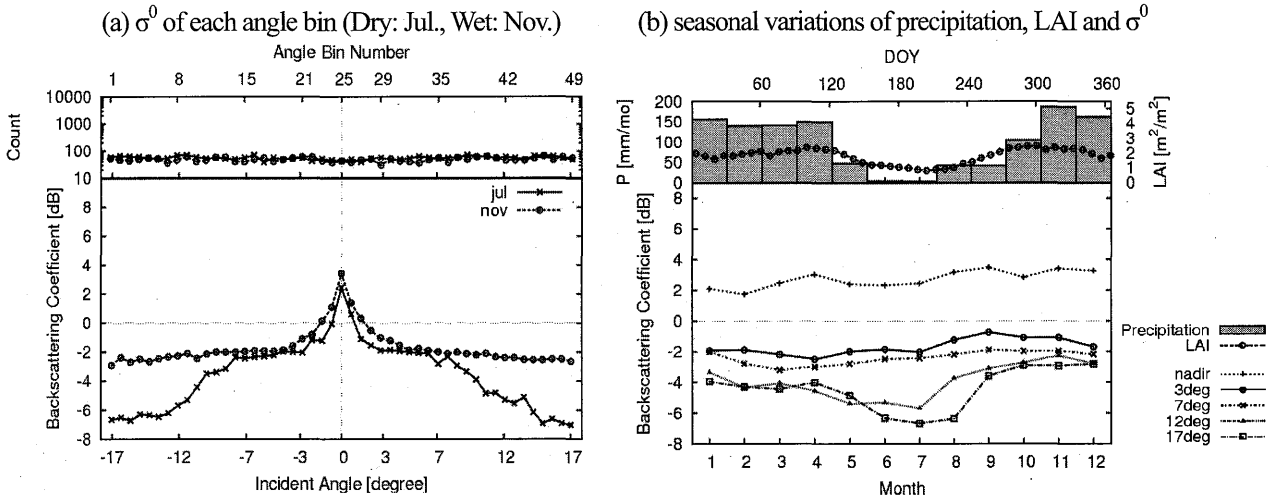

Fig. 4. The same as Fig. 2 but for woody savannas.

(a) Feature space

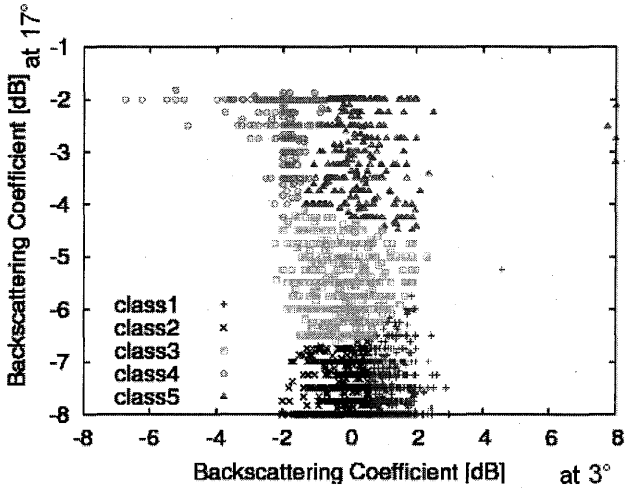

(b) Classification map by k-mean method

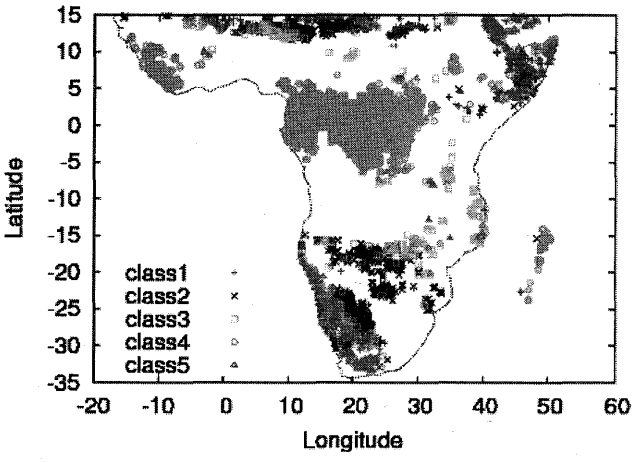

Fig. 5. Classification results using annual mean σ^0 at 3° and 17°. (a) feature space (the abscissa is σ^0 at 3°, the ordinate is σ^0 at 17°.), and (b) Classification map by k-mean method, k=5.

4. Conclusions

The incident angle dependency of σ^0 for woody savannas in the dry month is similar to that for savannas, but that in the rainy month is similar to that for ebf. The month of maximum σ^0 at nadir and 17° corresponds to that of precipitation. It implies that σ^0 is affected by soil moisture. On the other hand, the month of maximum ^{0} at 3° does not correspond to that of precipitation. It implies that σ^0 at 3° is susceptible to vegetation canopy. It suggests that the combination of 3° and 17° of σ^0 enable to classify vegetation land covers.

Acknowledgements

TRMM products were provided by the National Aeronautics and Space Administration (NASA) and the Japan Aerospace Exploration Agency (JAXA). MODIS products were provided by NASA.

References

1) T. Iguchi, T. Kozu, R. Meneghini, J. Awaka, and K. Okamoto: Rain-profiling algorithm for TRMM precipitation radar, J. Appl. Meteor., 39, pp. 2038-2052, 2000.

2) S. Seto, T. Nakaegawa, T. Oki, and K. Musiake: Characteristics of backscattering coefficients at different land covers observed by TRMM-PR, Annual Journal of Hydraulic Engineering, 43, pp. 223-226, 1999 (written in Japanese).

3) Y. Hirabayashi, S. Seto, S. Kanae, T. Oki, and K. Musiake: Analyses of global land cover information using backscattering coefficients by TRMM-PR, Annual Journal of Hydraulic Engineering, 44, pp. 259-264, 2000, (written in Japanese).

4) M. Satake and H. Hanado: Diurnal change of Amazon rain forest σ^0 observed by Ku-band spaceborne radar, IEEE Trans. Geosci. Remote Sens., 42 (6), pp. 1127-1134, 2004.

5) T. Kozu, T. Kawanishi, H. Kuroiwa, M. Kojima, K. Oikawa, H. Kumagai, K. Okamoto, M. Okumura, H. Nakatsuka, and K. Nishikawa: Development of precipitation radar onboard the Tropical Rainfall Measuring Mission (TRMM) satellite, IEEE Trans. Geosci. Remote Sens., 39 (1), pp. 102-116, 2001.

6) G. J. Huffman, R. F. Adler, D. T. Bolvin, G. Gu, E. J. Nelkin, K. P. Bowman, Y. Hong, E. F. Stocker, and D. B. Wolff: The TRMM multisatellite precipitation analysis (TMPA): Quasi-global, multiyear, combined-sensor precipitation estimates at fine scales, J. Hydrometeor., 8, pp. 38-55, 2006.

7) R. B. Myneni, S. Hoffman, Y. Knyazikhin, J. L. Privette, J. Glassy, Y. Tian, Y. Wang, X. Song, Y. Zhang, G. R. Smith, A. Lotsch, M. Friedl, J. T. Morisett, P. Votava, R. R. Nemani, and S. W. Running: Global products of vegetation leaf area and fraction absorbed PAR from year one of MODIS data, Remote Sens. Environ., 83, pp. 214-231, 2002.